

Phase transition temperatures of Sn–Zn–Al system and their comparison with calculated phase diagrams

Bedřich Smetana · Simona Zlá · Aleš Kroupa ·
Monika Žaludová · Jaromír Drápala ·
Rostislav Burkovič · Daniel Petlák

CEEC-TAC1 Conference Special Issue
© Akadémiai Kiadó, Budapest, Hungary 2012

Abstract The Sn–Zn–Al system was studied in connection with the possible substitution of lead-based solders for temperatures up to 350 °C. Ternary alloys with up to 3 wt% of aluminium were prepared. The investigated alloys lie close to the monovariant line (eutectic valley) of the Sn–Zn–Al system. The temperatures of phase transitions of six binary Sn–Zn reference alloys and fourteen ternary Sn–Zn–Al alloys using DTA method were investigated in this paper. DTA experiments were performed at the heating/cooling rate of 4 °C min⁻¹ using Setaram SETSYS 18_{TM} experimental equipment. The temperatures of phase transitions in the ternary Sn–Zn–Al system were obtained, namely, the temperature of ternary eutectic reaction T_{E1} (197.7 ± 0.7 °C), temperature of ternary transition reaction T_{U1} (278.6 ± 0.7 °C), temperatures of liquidus and other transition temperatures for studied alloys. Temperatures obtained during DTA heating runs were used as authoritative. DTA curves obtained during cooling enabled realising better differentiation of the obtained overlapped heat effects (peaks) during heating.

Theoretical isopleths of the Sn–Zn–Al phase diagram were calculated using the Thermocalc software and MP0602 thermodynamic database. Experimental data were compared with the calculated temperatures, and a good agreement was obtained.

Keywords Sn–Zn–Al system · DTA · Phase transition temperatures · Phase diagram calculation

Introduction

Sn–Zn–Al system is studied in connection with the worldwide search for materials which can play a role in high-temperature lead-free soldering for applications in electrical engineering and in automotive industry [1, 2]. It is particularly interesting because of low toxicity in comparison with the systems containing lead, of the increased anti-corrosion effects caused by the presence of Al, and also of other properties, such as surface tension, wettability, heat, and electric conductivity, structural and electrochemical properties. It is for these reasons that the Sn–Zn–Al system has been the focus of continuous investigation in the field of lead-free soldering. However, either there is a persistent lack of basic experimental data about this ternary system still, or the available data contradict each other [3–7]. This is caused mainly by considerable problems appearing during the experimental studies of this system. In this study, the investigation is focused on the area close to the monovariant line in the phase diagram of Sn–Zn–Al ternary system (Fig. 1). As this region of the Sn–Zn–Al phase diagram still deserves a lot of attention [3–11], the temperatures of phase transitions were measured in this region. Six binary Sn–Zn and 14 ternary Sn–Zn–Al alloys were studied. Experimental measurements were made using DTA method and Setaram

B. Smetana (✉) · S. Zlá · M. Žaludová
Department of Physical Chemistry and Theory of Technological Processes, Faculty of Metallurgy and Materials Engineering, VŠB-TU Ostrava, 17. listopadu 2172/15, Ostrava-Poruba, Czech Republic
e-mail: bedrich.smetana@vsb.cz

A. Kroupa
Institute of Physics of Materials, Academy of Sciences of the Czech Republic, Žitkova 22, Brno, Czech Republic

J. Drápala · R. Burkovič · D. Petlák
Department of Nonferrous Metals, Refining and Recycling, Faculty of Metallurgy and Materials Engineering, VSB-TU Ostrava, 17. listopadu 2172/15, Ostrava-Poruba, Czech Republic

Setsys 18_{TM} system. Results of experimental analyses were compared with the results of thermodynamic modelling using the Thermocalc software with the thermodynamic database compiled by some other authors within the framework of COST MP0602 project [12, 13].

Binary Sn–Zn, Al–Sn and Al–Zn systems

The knowledge of simpler systems is necessary for the characterisation of the behaviour of more complex systems. In the case of the Sn–Zn–Al system, the Sn–Zn, Al–Sn and Al–Zn binary systems have to be known (Fig. 2). The phase diagram of Zn–Sn binary system is a simple one of eutectic type [14]. The temperature of the eutectic reaction is 198.5 °C. Al–Sn system [14] is also a simple eutectic type with the eutectic reaction at 228.5 °C. Equilibrium Al–Zn phase diagram [14] comprises the eutectic reaction at 381 °C and eutectoid reaction at 277 °C.

Ternary Sn–Zn–Al system

Ternary Sn–Zn–Al system was investigated, and the obtained results were published elsewhere [3–11]. The theoretical thermodynamic description based on existing experimental data was published [3–7, 9, 10]. There are two important transition reactions in the system: eutectic reaction, and ternary transition reaction. The overview of experimentally measured temperatures of ternary eutectics (T_{E1}) and ternary transition reaction (T_{U1}) is shown in Tables 1, 2.

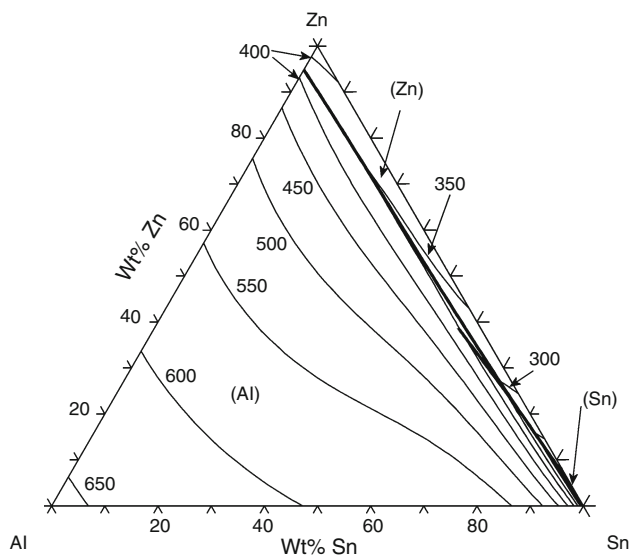


Fig. 1 Calculated Sn–Zn–Al equilibrium phase diagram using COST database [12], liquidus projection

Thermodynamic calculations

The thermodynamic descriptions of binary systems were taken from the previous studies by Fries et al. [8] for Al–Sn system; from Mey [15] for Al–Zn system; and from Fries [16] for Sn–Zn system. The thermodynamic modelling of

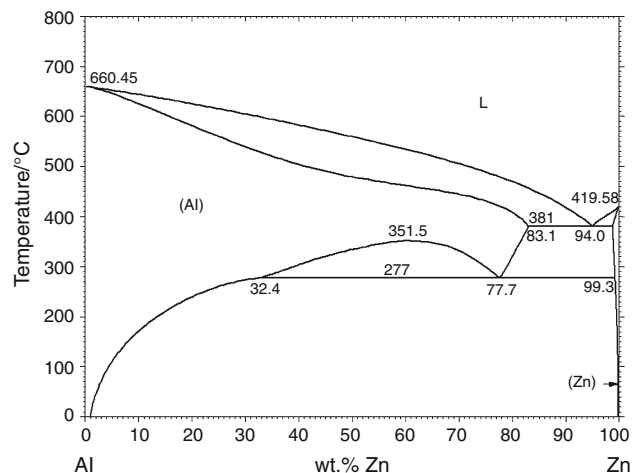
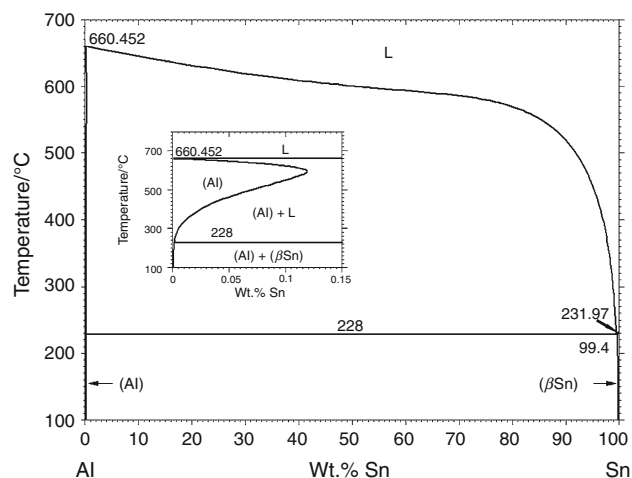
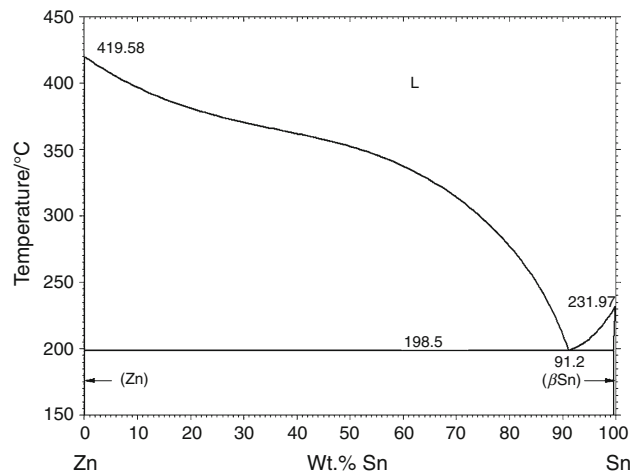


Fig. 2 Zn–Sn, Al–Sn and Al–Zn equilibrium phase diagrams, [14]

Table 1 Ternary eutectic reaction scheme

Reaction	$T/^\circ\text{C}$	Phase	Composition/wt%			Ref.	
			Al	Zn	Sn		
$L \leftrightarrow (Al) + (Zn) + (Sn)$	E_1	L	0.8	6.3	92.9	[3]	
		L	1.5	10.4	88.1	[4]	
		L	0.6	7.7	91.7	[5]	
		L	0.6	9.0	90.4	[6]	
		L	197.0			[7]	
		L	195.4			[8]	
		(Al)		87.4	12.6	0.0	
		(Zn)		0.2	99.6	0.2	
		(Sn)		0.2	0.3	99.5	
			197.0				[9]
			196.0				[10]
	197.0				[11]		

L Liquid phase, *Al* solid solution of Al, *Zn* solid solution of Zn, *Sn* solid solution of Sn

Table 2 Ternary invariant reaction scheme

Reaction	$T/^\circ\text{C}$	Phase	Composition/wt%			Ref.
			Al	Zn	Sn	
$L + (Al)' \leftrightarrow (Al)'' + (Zn)$	U_1	L	1.82	21.70	76.48	[8]
		(Al)'	22.30	77.65	0.05	
		(Al)''	71.41	28.58	<0.01	
		(Zn)	0.67	99.04	0.29	
			278.0			
	275–276				[10]	
	278.0				[11]	

L Liquid phase, *Al'* solid solution with low Al content, *Al''* solid solution with high Al content, *Zn* solid solution of Zn

the Sn–Zn–Al system is based on the thermodynamic dataset published by Fries et al. in [8]. The above mentioned thermodynamic assessments were compiled as a part of the COST MP0602 database [12], created in the scope of the COST MP0602 Action [17]. The 4.4 version of the SGTE database for the Gibbs energies of pure elements (the so-called unary data) [18] was used in the COST MP0602 database, and therefore all the above mentioned systems were tested for consistency with respect to the new version of the SGTE database. It was found that the system Al–Sn had to be reassessed in the scope of the MP0602 database as the difference between the Gibbs energy of Sn in fcc_A1 structure (metastable) and Sn in bct_A5 (stable) structure was different in version 4.4. of the SGTE database in comparison with the value from [19], used by Fries et al. [8]. The phase diagram using the updated thermodynamic data for Al–Sn from [12] is identical with the one produced by the older assessment [8], and therefore the same diagram can be used in the modelling of the ternary Sn–Zn–Al system.

The solid phases existing in the Sn–Zn–Al system are modelled as substitutional solid solutions. The bct_A5 (Sn), hcp_A3 (Zn) with modified c/a ratio and fcc_A1 (Al) phases exist in the system. There is an fcc_A1 miscibility gap in the binary Al–Zn system which extends into the ternary phase diagram. The liquid phase is also modelled using the substitutional solution model. No intermediate phase exists in the system.

Experiment

Sample preparation

Pure metals (Sn 4N5, Zn 4N and Al 3N5) were used for the preparation of alloys with defined composition. Chemical purification was applied to the pure metals to remove surface oxides layers. The binary (B1–B6, Table 3) and selected ternary compositions (A5, A6, A8, A10, A11, A13 and A14: Table 4) were prepared by

melting in a resistance furnace in a graphite crucible. Alloys were air cooled. Ingots weighing approx. 100 g were prepared (in some cases 200 g). Very small particles

of Al_2O_3 were observed in some alloys prepared in graphite crucibles. This fact could negatively influence the obtained results.

Table 3 The temperatures of phase transitions in binary alloys

Solder	Composition/wt%	Heating (exp.)		Calculated	
		Temperature/°C		Temperature/°C	
		T_E	T_L	T_E	T_L
B1	12.4Sn87.6Zn	198.8	397.1	198.6	392.1
B2	30.8Sn69.2Zn	199.2	382.0	198.6	373.0
B3	54.5Sn45.5Zn	199.5	357.3	198.6	354.0
B4	66.6Sn33.4Zn	198.9	323.5	198.6	329.5
B5	83.3Sn16.7Zn	198.0	272.6	198.6	263.5
B6	91.1Sn8.9Zn	197.9	–	198.6	208.1

T_E Eutectic reaction temperature, T_L liquidus temperature

Table 4 The temperatures of phase transitions in ternary alloys, T_{E1} , T_1 , T_2 , T_{U1} , T_3 , T_4 , T_5 , T_6 , T_L

Solder	Composition/wt%		Temperature/°C								
			T_{E1}	T_1	T_2	T_{U1}	T_3	T_4	T_5	T_6	T_L
A1	89.9Sn 9.7Zn 0.4Al	exp.	199.1								–
		teor.	195.4								210.3
A2	85.2Sn 14.5Zn 0.4Al	exp.	197.5								253.4
		teor.	195.4								245.9
A3	76.8Sn 22.7Zn 0.5Al	exp.	198.2								296.3
		teor.	195.4								289.8
A4	86.5Sn 12.9Zn 0.6Al	exp.	197.4								239.2
		teor.	195.4								233.8
A5	88.8Sn 10.2Zn 1.0Al	exp.	196.6		207.1						263.0
		teor.	195.4		211.1						241.7
A6	94.8Sn 4.2Zn 1.0Al	exp.	196.9	215.1							268.0
		teor.	195.4	210.5							266.9
A7	69.9Sn 28.5Zn 1.6Al	exp.	197.1						277.5		325.2
		teor.	195.4						272.8		307.2
A8	82.2Sn 16.0Zn 1.8Al	exp.	197.5		258.1						324.3
		teor.	195.4		249.2						284.7
A9	70.2Sn 28.0Zn 1.8Al	exp.	197.8			277.5					313.5
		teor.	195.4			277.9					304.5
A10	90.8Sn 6.7Zn 2.5Al	exp.	198.4	207.8							379.4
		teor.	195.4	201.2							376.4
A11	76.2Sn 21.0Zn 2.8Al	exp.	197.4			279.8	285.1				342.2
		teor.	195.4		274.4	–	–				342.7
A12	68.2Sn 29.0Zn 2.8Al	exp.	197.6			277.8				311.5	336.4
		teor.	195.4			277.9				316.7	317.1
A13	69.7Sn 27.4Zn 2.8Al	exp.	197.6			279.1	310.2				333.0
		teor.	195.4			277.9	306.5				318.2
A14	59.0Sn 38.0Zn 3.0Al	exp.	197.8			278.7		324.0			348.5
		teor.	195.4			277.9		326.0			329.8

The second set of ternary samples was prepared in the evacuated (sealed) quartz ampoules (A1–A4, A7, A9, and A12, Table 4) to avoid possible oxidation. Pieces of pure metals were melted and held at 750 °C for sufficiently long time to secure their complete melting and homogenisation of samples. Samples in evacuated ampoules were slowly cooled to secure state close to equilibrium of prepared alloys. The mass of the prepared samples was 200 g.

DTA-method: experimental conditions

The cubes with approximate dimensions $2 \times 2 \times 2$ mm were cut from the as-cast ingots for DTA analyses. The mass of the analysed samples was in the range from 100 to 150 mg. Differential thermal analysis of the investigated alloys was carried out in the inert dynamic atmosphere of purified Ar (purity > 99.9999 %, gas flow rate was 2 l h^{-1}). Corundum crucibles were used for the analyses. Instrument was calibrated before measurement with respect to the melting temperatures of the standard metals with 5 N purity (In, Sn, Bi, Pb, Zn).

Two or three cycles of heating and cooling at the rate of 4 °C min^{-1} for each sample were realised. Temperature range of the performed analyses was from the room temperature to 450 °C (the maximum temperature was appropriately lowered for alloys with lower liquidus temperature to avoid possible oxidation and evaporation). The first cycle started at the ambient temperature up to the maximum temperature of 450 °C; it was then followed by cooling to 50 °C and repetitive heating from 50 to 450 °C. Comparison of DTA curves for the first, the second and the third heating runs for the studied samples is presented in Fig. 3. The curves obtained during the second and third cycles are almost identical, but DTA curve obtained at the first heating shows small deviations in comparison with those of the second and

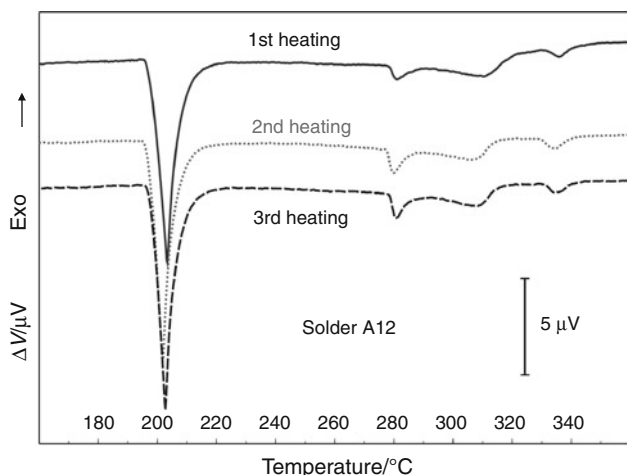


Fig. 3 DTA heating curves obtained during three repeated DTA runs, alloy A12

third DTA runs. This is probably caused by poorer thermal contact between the sample and crucible during the first run. Only transition temperatures from the second and third heating cycles were used for the evaluation. The results are shown in Tables 3, 4. Mean values of binary eutectic temperature, ternary eutectic temperature and ternary transition reaction temperatures from the second and third heating runs were calculated: $T_E = 198.7$; $T_{E1} = 197.7$ and $T_{U1} = 278.6$. Very good reproducibility of results for invariant temperatures was obtained, and standard deviation was determined to be $\delta = \pm 0.7 \text{ °C}$ for measurements of these three temperatures.

Phase transition temperatures obtained at cooling process are significantly shifted to lower values. The nucleation problem is the reason for this undercooling. The initiation and further growth of critical nuclei are very difficult. The homogeneous nucleation at cooling process is supposed to be according to some authors [20], and therefore the temperatures obtained at cooling are not suitable for phase diagrams construction. Nevertheless, the curves obtained during cooling can be still very helpful during analysis of the DTA heating curves. During cooling, we can often distinguish better the peaks demonstrating very small and/or overlapping heat effects (peaks) in the samples, particularly such transformation effects, which exist in close proximity and cannot be easily analysed on heating curves. It is therefore possible to analyse even diminutive changes of the DTA curves (during heating) and attribute them to relevant phase transformation (Figs. 4, 6).

Results and discussion

The examples of DTA curves (second heating and cooling run) obtained for the binary Sn–Zn alloys are shown in Fig. 4. Characteristic phase transitions temperatures of binary alloys are summarised in Table 3. Eutectic reaction and liquidus temperatures (T_E and T_L) are presented. Comparison of our experimental results with calculated Sn–Zn binary phase diagram is shown in Fig. 5.

Figure 6 shows the curves (also for the second runs) obtained for the ternary Sn–Zn–Al alloys A1–A14. Characteristic temperatures of phase transitions for these alloys are given in Table 4. The indexes x (T_x) for the phase transitions temperatures are explained in Table 5.

Transition temperatures of binary Sn–Zn alloys

Two thermal effects (peaks) were observed on all curves except B6, which correspond to the expected phase transitions (Fig. 4). The first peak is characterised by its steep inclination both at heating and at cooling. Such peak shape corresponds to an invariant reaction. Peaks observed in this study match the

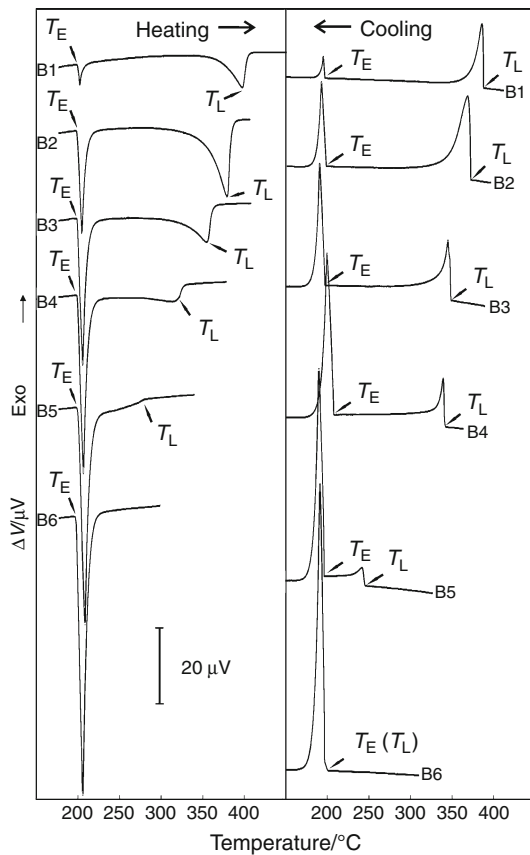


Fig. 4 Comparison of heating and cooling DTA curves for binary alloys B1–B6

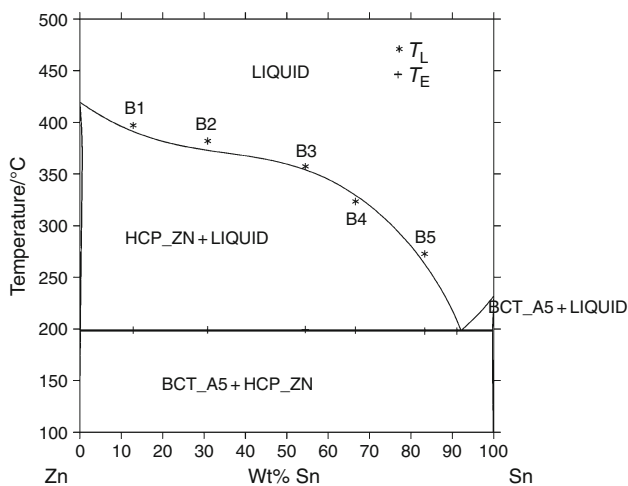


Fig. 5 Comparison of experimental temperatures of phase transitions for binary alloys B1–B6 with calculated Sn–Zn phase diagram using COST database [12]

eutectic reaction in the binary Sn–Zn system. The obtained mean eutectic temperature $T_E = 198.7 \pm 0.7$ °C of studied alloys B1–B6 corresponds very well to the calculated value for Sn–Zn phase diagram (see Fig. 5; Table 3).

The second peak corresponds to the complete melting of the solid phase (on heating curve, at cooling process corresponds to the first stage of solidification) in the binary alloys. Temperature of liquidus T_L varies, depending on composition of alloy, in the range of 397.1–197.9 °C.

Alloy B6 exhibits the eutectic composition. Only one thermal effect was detected at the heating and cooling curves. Its presence demonstrates that B6 alloy goes through a eutectic invariant reaction.

Liquidus temperatures of B1–B5 alloys evaluated from the DTA curves are generally in good agreement (except liquidus temperature for the samples B2 and B5) with the calculated liquidus curve of Sn–Zn diagram (Fig. 5). The shift of T_L for sample B2 (discrepancy with calculated Sn–Zn phase diagram) could be probably caused by deviation in chemical composition determination. In the case of B5 sample, the signal for the liquidus temperature is very weak (see Fig. 4, corresponding to the steep slope of the curve) and therefore the uncertainty of the reading is greater. Other temperatures measured (especially the eutectic temperature) are also in very good agreement with the accepted assessment of Sn–Zn phase diagram [16].

Very good agreement between the measured values in this study and those in [14] for the eutectic temperature T_E and liquidus temperatures T_L (except T_L for B2 and B5) confirm good quality of the prepared samples, proper setting of experimental device and the method of evaluation. Therefore the results for ternary system, obtained by the same experimental procedure can be accepted as reliable for the comparison with theoretical calculation.

Transition temperatures of ternary Sn–Zn–Al alloys

Up to four thermal effects corresponding to phase transitions and relevant phase transition temperatures were observed in ternary alloys (see Fig. 6; Table 4).

The particular transition temperatures in Fig. 6 and tables were labelled in a consistent way, which is defined in Table 5.

The experimentally obtained temperatures of phase transitions are shown in theoretically calculated isopleths of the Sn–Zn–Al phase diagram for the contents of Al = 0.5, 1, 1.5, 2 and 3 wt% (Figs. 7, 8). The isopleths were calculated using the MP0602 thermodynamic database developed in the scope of COST MP0602 Action [12].

The comparison of the experimentally measured phase transition temperatures for alloys A1–A4 with theoretically predicted values for relevant isopleth (0.5 wt%) is shown in Fig. 7. Excellent agreement between experimental and theoretical transition temperatures was achieved. Two thermal effects were observed for ternary alloys A2–A4. Only one thermal effect corresponding to the ternary eutectic reaction was observed for alloy T_1 , and

Fig. 6 Comparison of heating and cooling DTA curves for ternary alloys A1–A14

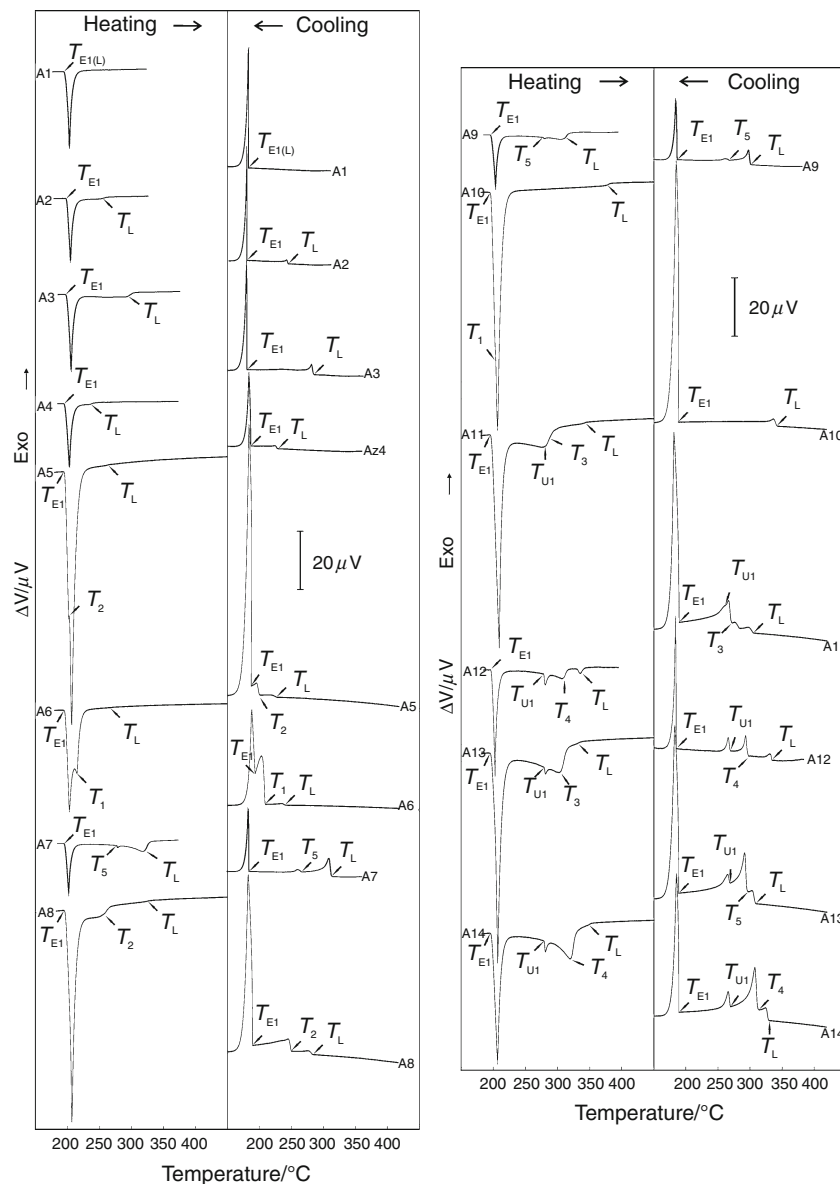


Table 5 Labeling of the transition temperatures in ternary alloys, T_{E1} , T_1 , T_2 , T_{U1} , T_3 , T_4 , T_5 , T_6 , T_L

Designation	Transition (end)
T_{E1}	$L \leftrightarrow (Al) + (Zn) + (Sn)$
T_1	$L + (Al)'' + (Sn) \rightarrow L + (Al)''$
T_2	$(Zn) + (Al)'' + L \rightarrow L + (Al)''$
T_{U1}	$L + (Al)' \leftrightarrow (Al)'' + (Zn)$
T_3	$L + (Al)' + (Al)'' \rightarrow L + (Al)''$
T_4	$L + (Zn) + (Al)' \rightarrow L + (Al)'$
T_5	$(Zn) + (Al)'' + L \rightarrow L + (Zn)$
T_6	$L + (Al)' \rightarrow L + (Al)' + (Al)''$
T_L	Temp. of liquidus

temperature of the reaction (T_{E1}) was evaluated. Composition of this alloy corresponds to the ternary eutectic concentration.

The isopleth for 1 wt% of Al is presented in Fig. 7 also. Three thermal effects were observed and phase transition temperatures evaluated for relevant experimental samples. Temperature of ternary eutectic reaction is again in very good agreement with calculated one. Experimental and theoretical temperatures T_1 (for sample A6) and T_2 (for sample A5, see Table 5 for labelling) are also in excellent agreement. Experimental liquidus temperature of sample A6 lies on the liquidus curve of the isopleth section of the phase diagram and T_L of sample A5 is positioned slightly higher.

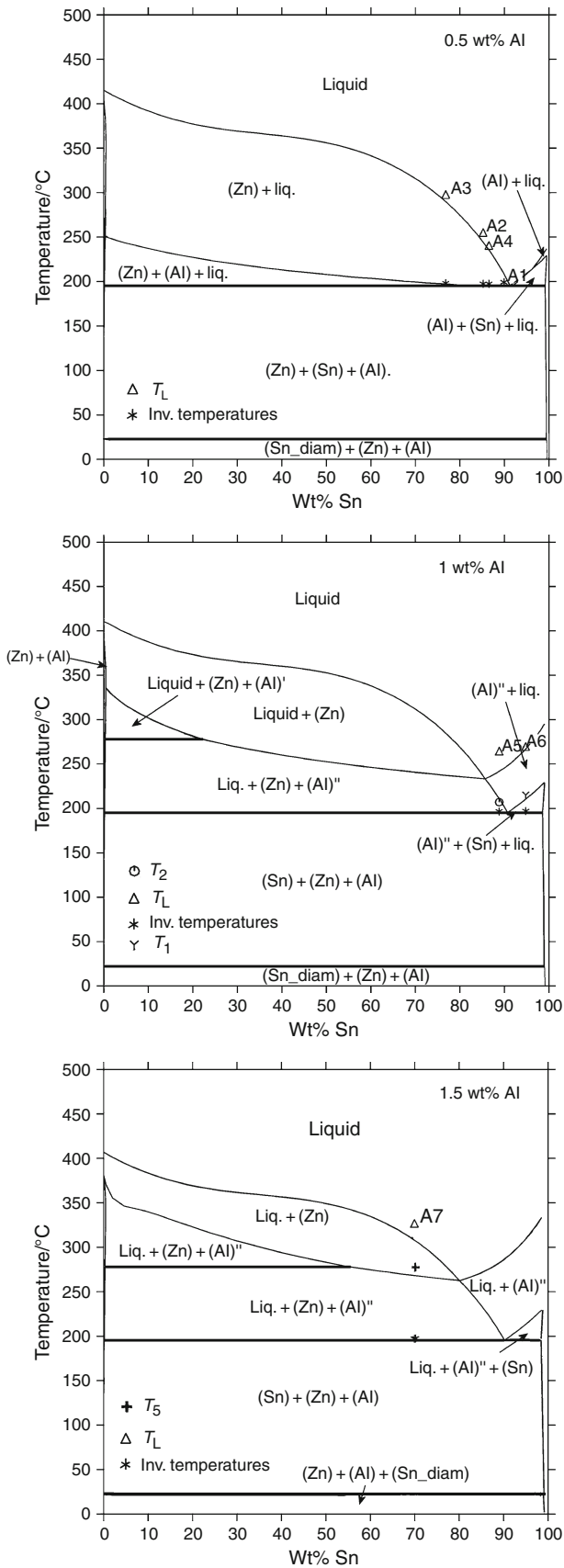


Fig. 7 Comparison of experimental temperatures of phase transitions of ternary alloys A1–A7 with theoretically calculated isopleths of the Sn–Zn–Al phase diagram for 0.5, 1.0 and 1.5 wt% Al

Temperatures of phase transitions of ternary alloy A7 are presented in Fig. 7 (1.5 wt%). The greatest difference was observed for liquidus temperatures, but even in this case, the difference does not exceed 18 degrees of Celsius. Here the difference can be caused because of small differences of the Al contents in our samples—meaning that

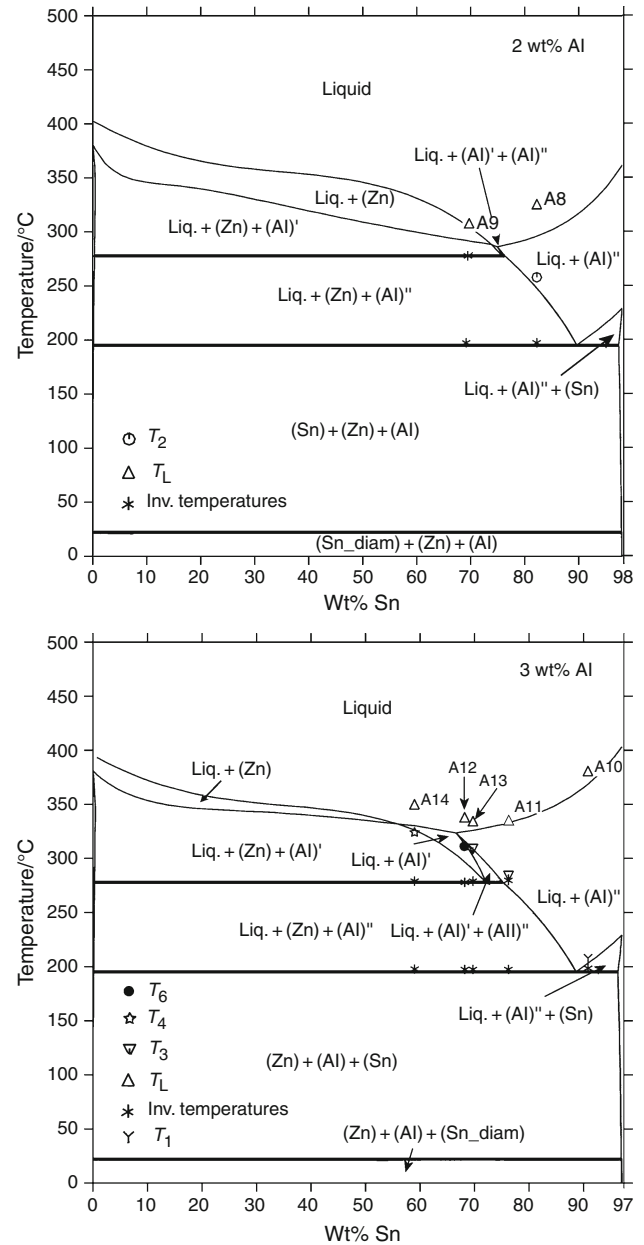


Fig. 8 Comparison of experimental temperatures of phase transitions of ternary alloys A8–A14 with theoretically calculated isopleths of the Sn–Zn–Al phase diagram for 2.0 and 3.0 wt% Al

our experimental composition does not lie exactly on the calculated isopleth section. Almost no deviations were observed in the case of temperatures T_5 and T_{E1} .

Three thermal effects were also observed for alloys A8 and A9 (Fig. 6). Comparison with theoretical calculations is shown in Fig. 8. End of melting (T_L) was observed above liquidus line of the isopleth (2 wt% of Al), slightly for A9 and about 39 °C for A8. Temperatures T_{E1} , T_5 and T_2 agree well with calculated lines of Sn–Zn–Al diagram.

The experimentally obtained transition temperatures for samples A10–A14 are presented in the calculated isopleth for 3 wt% of Al in Fig. 8. Excellent agreement was achieved in the case of ternary transition reaction temperatures. The largest deviations (max. about 20 °C) were observed in the case of T_L for samples A12, A14.

The mean experimental value of T_{E1} (197.7 ± 0.7 °C) was calculated on the base of all T_{E1} temperatures obtained at second and third DTA heating run. Temperature T_{E1} is very close to the values presented in [6] and [5], Table 1. The highest difference (2.3 K) was observed between experimental value obtained in this study and the calculated value in our work and in [8] (Table 1). As the thermodynamic data used for the calculations are based on [8], these results showed that the reassessment done because of different unary data used in the MP0602 database in comparison with [8] was correct.

The mean value of T_{U1} is 278.6 ± 0.7 °C (calculated from second and third heating runs of all the samples). Experimental value obtained in this work is about 0.7 °C higher than the temperature value obtained by calculations here ($T_{U1} = 277.9$ °C) and about 0.8 °C higher than the temperature in [8] (Table 2). The highest difference (3.6 K) was observed between the value obtained in this work and value presented in [10].

Above mentioned differences between the experimentally measured and calculated transition temperatures, observed in some cases, can be caused partially by the insufficient homogeneity of some analysed samples (chemical and structural; composition of small pieces prepared for DTA could, in some cases, slightly differ from that composition obtained by chemical analysis of ingots—pieces of alloys for DTA were not taken exactly from the same place like the performed chemical analysis). Micro-particles of Al_2O_3 were present in some alloys (identified in as-cast samples). This fact could have some influence, too.

Also the Al content in some alloys did not correspond accurately to the compositions of calculated isopleths and therefore transition temperatures could be shifted. It was found (it is apparent) that a very small change in chemical composition can significantly shift the phase transition temperatures T_1 – T_6 and T_L .

Further attention will be paid to the alloys in the concentration range of 65–80 wt% Sn and 3 wt% Al in the

future studies. Several phase transitions take place in this concentration region and therefore it is not easy to identify the overlapping heat effects on the DTA curve and to assign corresponding phase transition to the heat effects.

There is rather poor agreement for some ternary alloys in comparison with the binary ones, and the difference can be considerable in some cases. Here the experimental errors in composition measurements can play more significant role, especially because of low amount of Al. Even small error can influence the agreement with theoretically calculated values.

In some cases also the transition temperatures are very close to each others. This is the case of the eutectic temperature reading for A1–A6 alloys and even more pronounced situation is for the alloys A11–A14, where often two transitions temperatures are so close, that they cannot be separated on the experimental DTA curves, but the reading is influenced by it.

Also, the signals corresponding to the liquidus temperatures T_L are significantly less distinct and the uncertainty of the reading is greater (this is true also for the binary sample B5, which exhibits also large deviation in comparison with theoretical value).

Conclusions

Following conclusions were formulated on the basis of obtained experimental results from DTA measurements, realised using the Setaram SETSYS 18_{TM} thermal analysis system.

For binary Sn–Zn alloys:

- Temperature of eutectic reaction T_E of investigated binary alloys Sn–Zn was found to be 198.7 ± 0.7 °C, and is in excellent agreement with the widely accepted temperature of eutectic reaction (198.5 °C) [14]. This finding confirms the proper experimental setup of the apparatus and correct evaluation of DTA curves to be used for studying ternary systems.
- Temperatures of liquidus T_L of binary alloys, obtained from the heating curves, were slightly higher (except T_L for B4) than in the published Sn–Zn binary system [14] (this may be caused by delay of heat transfer in the sample, because of limited thermal conductivity of the sample).

For ternary Sn–Zn alloys:

- The temperature of ternary eutectic reaction T_{E1} in the Sn–Zn–Al system was found to be 197.7 ± 0.7 °C, this value is very close mainly to the value presented in [6], 198.0 °C and [5], 197.3 °C. The highest difference (2.3 K) was observed between value obtained in this study and calculated values here and in work [8].

- The mean value of T_{U1} temperature was found to be 278.6 ± 0.7 °C. Experimental value obtained in this work is about 0.7 °C higher than the calculated temperature value presented in this study and in [8]. The highest difference (3.6 K) was observed between the value obtained in this work and value presented in [10].
- Other phase transitions were observed in ternary alloys above the eutectic reaction, and a majority of these phase transition temperatures, e.g. liquidus temperatures, are in an excellent agreement with thermodynamic calculations.
- The DTA cooling curves allowed us to distinguish some overlapping thermal effects (peaks) better.

New original experimental data were obtained in this study. Comparison of experimental and theoretical data was performed in this study. The experimental data confirmed the quality of the theoretical assessment of the Sn–Zn–Al system based on the study of Fries et al. [8] and reassessed by the authors in the scope of the development of the COST MP0602 database.

Acknowledgements This study was carried out in the scope of the projects COST MP0602 (European Concerted Action) and by the Ministry of Education, Youth and Sports of the Czech Republic (Projects Nos. OC08032, OC08053 and MSM 6198910013). The calculations were performed by Thermocalc software package. The authors are grateful to Dr. A. Watson from University of Leeds for performing selected calculations.

References

1. Gomidželović L, Živković D, Kostov A, Mitovski A, Balanović L. Comparative thermodynamic study of Ga–In–Sb system. *J Therm Anal Calorim.* 2011;103:1105–9.
2. Amore S, Delsante S, Parodi N, Borzone G. Calorimetric investigation of the Cu–Sn–Bi lead-free solder system. *J Therm Anal Calorim.* 2008;92:227–32.
3. Plumbridge DV. On the Binary and Ternary Alloys of Aluminum, Zinc, Cadmium and Tin (in German). Thesis. University of München, Germany; 1911.
4. Losana L, Carozzi E. The ternary alloys of aluminium–zinc and tin (in Italian). *Gazz Chim Ital.* 1923;53:546–55.
5. Prowans S, Bohatyrewicz M. Układ aluminium–cyna–cynk. *Arch Hutn.* 1968;13:217–33.
6. Nayak AK. Constitution of ternary Al–Zn–Sn alloys determined by an iso-peribol calorimeter. *Trans Indian Inst Met.* 1975;28:285–90.
7. Vincent D, Sebaoun A. Study of the Aluminum–Zinc–Tin Ternary System (in French). *J Therm Anal.* 1981;20:419–33.
8. Fries SG, Lukas HL, Kuang S, Effenberg G. Calculation of the Al–Zn–Sn ternary system. In: Hayes F, editor. *User aspects of phase diagrams.* London: The Institute of Metals; 1991. p. 280–6.
9. Aragon E, Sebaoun A. Al–Zn–Sn phase diagram. X-ray diffraction study at various temperatures. *J Therm Anal Calorim.* 1998;52: 523–35.
10. Aragon E, Vincent D, Zahra AM, Sebaoun A. Al–Zn–Sn phase diagram. Calorimetric study of the isobaric invariants. *J Therm Anal Calorim.* 1999;55:271–82.
11. Vincent D. Contribution a l'Etude du systeme ternaire Al–Zn–Sn. Thesis, No. 81, Université Claude Bernard, Lyon I. France; 1982.
12. Dinsdale AT, Watson A, Kroupa A, Vřešťál J, Zemanová A, Vízdal J. MP0602, thermodynamic database for high-temperature lead free solder systems compiled in the frame of COST MP0602 Action; 2007–2011.
13. Dinsdale AT, Watson A, Kroupa A, Vřešťál J, Zemanová A, Vízdal J. Atlas of phase diagrams for lead-free soldering. Brno: COST office; 2008.
14. Massalski TB, Okamoto H. Binary alloy phase diagrams. American Society for Metals, editor. Second edition plus updates on CD-ROM. Ohio; 1996.
15. an Mey S. Reevaluation of the Al–Zn system. *Z Metallkd.* 1993; 84(7):451–455.
16. Fries SG. Unpublished work. 2002.
17. Kroupa A. Cost COST Action MP0602—advanced solder materials for high temperature application (HISOLD) http://w3.cost.esf.org/index.php?id=248&action_number=MP0602.
18. Dinsdale AT. SGTE Unary database, version 4.4. www.sgte.org.
19. Dinsdale AT. SGTE data for pure elements. *Calphad.* 1991; 15:317–425.
20. Boettinger WJ, Kattner UR, Moon KW, Perepezko JH. Recommended practice guide: DTA & heat-flux DSC measurement of alloy melting and freezing. Washington: National Institute of Standards and Technology; 2006.